

## Supplementary information

Shape morphing of anisotropy-encoded tough hydrogels enabled by the asymmetrically-induced swelling and site-specifically mechanical strengthening

*Xiaohu Zhou,<sup>1,2#</sup> Tianzhen Li,<sup>1#</sup> Jiahui Wang,<sup>1#</sup> Fan Chen,<sup>1</sup> Dan Zhou,<sup>1</sup> Qi Liu,<sup>2</sup> Liyun Zhang,<sup>1</sup> Jiayan Shen,<sup>1</sup> Xuechang Zhou<sup>1,\*</sup>*

<sup>1</sup>College of Chemistry and Environmental Engineering, Shenzhen University, Shenzhen 518060, P. R. China

<sup>2</sup>Department of Chemistry, The Chinese University of Hong Kong, Shatin, N.T., Hong Kong SAR, P. R. China

\*Correspondence and requests for materials should be addressed to X. C. Z. (email: [xczhou@szu.edu.cn](mailto:xczhou@szu.edu.cn))

## Experimental Section

Materials:

Sodium alginate was purchased from Aladdin. Acrylamide and ammonium persulfate (APS) and calcium sulfate dihydrate ( $\text{CaSO}_4 \cdot 2\text{H}_2\text{O}$ ) were purchased from Macklin. N,N'-Methylenebisacrylamide (MBAA) and N,N,N',N'-tetramethylethylenediamine (TEMED) were purchased from Sigma-Aldrich. Ferric chloride hexahydrate ( $\text{FeCl}_3 \cdot 6\text{H}_2\text{O}$ ) was purchased from Fisher chemical. Advantec No. 2 filter paper was used for the ion transfer printing.

Ca-alginate/PAAm tough hydrogel synthesis

Sodium alginate (0.25 g) and acrylamide (2.00 g) were dissolved in 12.5 mL deionized water. After degassing for 2 hours, 60  $\mu\text{L}$  0.10 g/mL ammonium

persulphate (APS) aqueous solution as photothermal initiator, 96  $\mu\text{L}$  0.025 g/mL N, N'-methylenebisacrylamide (MBAA) aqueous solution as crosslinking agent, and 10  $\mu\text{L}$  N,N,N',N'-tetramethylethylenediamine (TEMED) as crosslinking accelerator were added to the former solution. Subsequently, 4 mL calcium sulfate ( $\text{CaSO}_4 \cdot 2\text{H}_2\text{O}$ , 0.0221 g) aqueous slurry was added as the ionic crosslinker for alginate. The resulting solution was poured into a plastic container, and cured with UV light at a wavelength of 254 nm (25 W, ZF-5, Shanghaijiapeng) at 55 °C for 1.5 h. Subsequently, the cured mixture was left in a humid box for several hours to stabilize the reactions.

#### Ferric ion transfer printing

To precisely control the ion penetration depth, the wetness of the ferric ion-dyed filter paper was controlled. 1 M ferric chloride solution was used for ion transfer printing. Filter papers cut into different patterns were first immersed in the ferric solution for dyeing for seconds; then, a towel tissue was placed on the paper slightly to absorb the free water in the paper. After depleting the free water, the transfer paper dyed with ferric ions could be placed on the tough gel for transfer printing immediately. The transfer printing time was controlled from 20 seconds to 5 minutes in current work.

The filter paper pattern was cut by scissors. The filter paper strips with the width of 2 mm and different length (5, 10, 15, 20 and 25 mm) were applied to the one-dimensional bending, swelling-induced helix experiments. The paper strips with 4 mm wide and 30 mm long were applied to the swelling-induced saddle-like structure.

The paper strips with 3 mm wide and 15 mm were applied to the tetrahedron structure. The filter paper flower was cut from 50 mm \* 50 mm square. Volume expansion ratio measurement

The Ca-alginate/PAAm tough gel round plates (diameter: 10 mm, thickness: 2 mm) was prepared by following the protocol mentioned above. Then, we immersed the round plates into the ferric chloride solutions with different concentrations to prepare the ferric encoded tough gel. After 3 hours incubation, we took out the gel plates and removed the free solutions on gels with the tissues. At last, we placed each gel plate into 20 ml DI water for swelling and weighed the weight of each gel plates after certain intervals.

#### Penetration Depth and Bending Angle Measurements

The patterned gels were observed under a microscope (Leica MZ 16, Germany) equipped with a charge-coupled device camera (SPOT Insight, Diagnostic Instruments). The penetration depths and bending angles of the gel were measured with photographs by ImageJ (NIH). As the ferric ion patterned part of the gel was brown, we measured the penetration depth by color analysis. Because the ferric ion concentration in the gel was continuously and dynamically changing due to diffusion and the boundary of the patterned and unpatterned parts was not sharp, the penetration depth was roughly measured. During the swelling process, the unpatterned calcium layer would expand to a large degree, while the patterned ferric layer would not change much. To more precisely measure the bending angle, we measured the angle based on the less changed ferric layer. However, during the swelling, the swollen

parts of the calcium layer at the terminals would contact each first to form the closed ring. Therefore, the measured bending angle could a little bit smaller than 360 degrees (Fig. 2c).

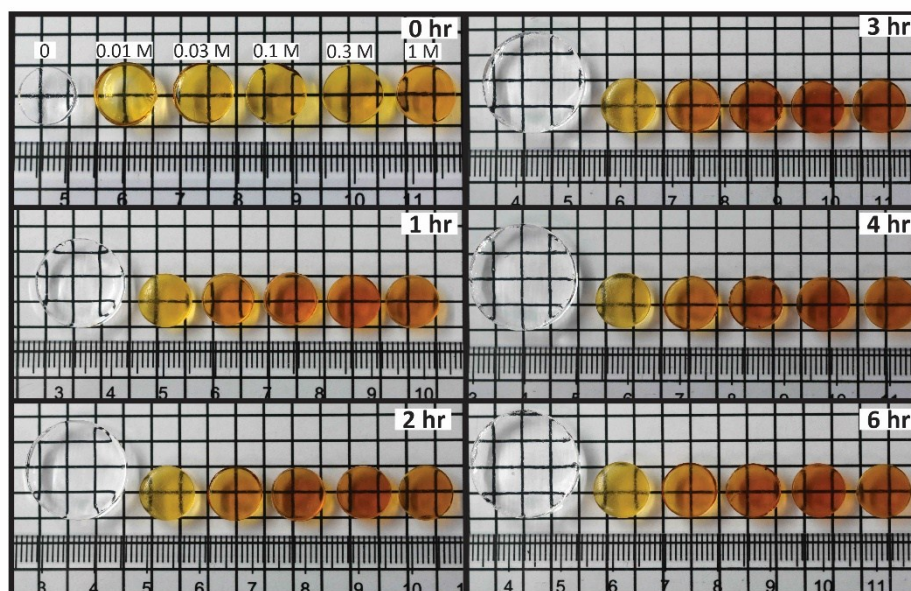


Fig. S1 Sequential photos of the tough gel in swelling.

Table S1 The volume change of the tough gel round plates after each step for the swelling kinetics measurement.

[Fe <sup>3+</sup> ]	volume change after incubation with ferric solution	volume change after swelling	overall volume change
0.01	1.3395	1.1061	1.4816
0.03	1.1502	1.0644	1.2242
0.1	1.1667	0.9859	1.1502
0.3	1.2160	0.9119	1.1089
1	1.2016	0.8458	1.0163

Supplementary Movie S1: Movie was compiled from time-lapse imagery every one minute for 128 min, and played at 7 fps (420X speed).

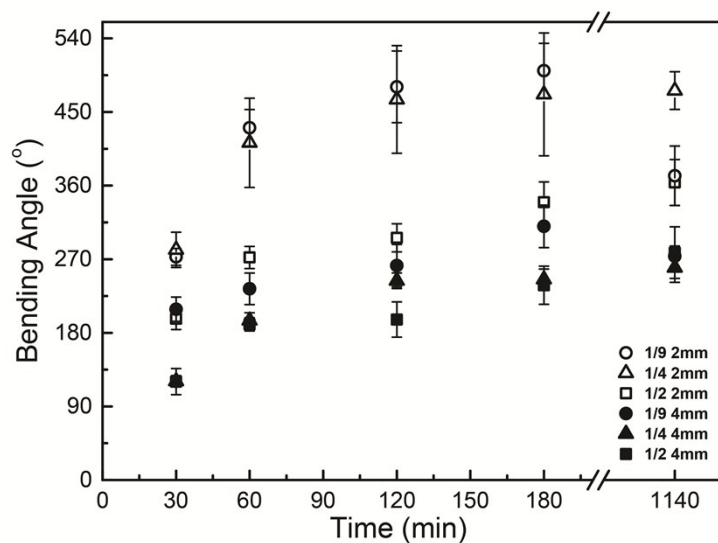


Fig. S2 Bending behavior of the hydrogels strips with different thickness and ferric-to-calcium layer ratio. The thin gel strips with the high surface-to-volume ratio would have the faster and larger bending behavior. The smaller ferric-to-calcium layer ratio would generate the faster and larger bending behavior. The bending angle decrease of the 2 mm thick gel strip with the layer ratio of 1/9 was due to the steric effect during the bending process. (Dimensions of the gel strips: 23 mm (long) \* 2 mm or 4 mm (thick) \* 1.5 ~ 2 mm (wide).)

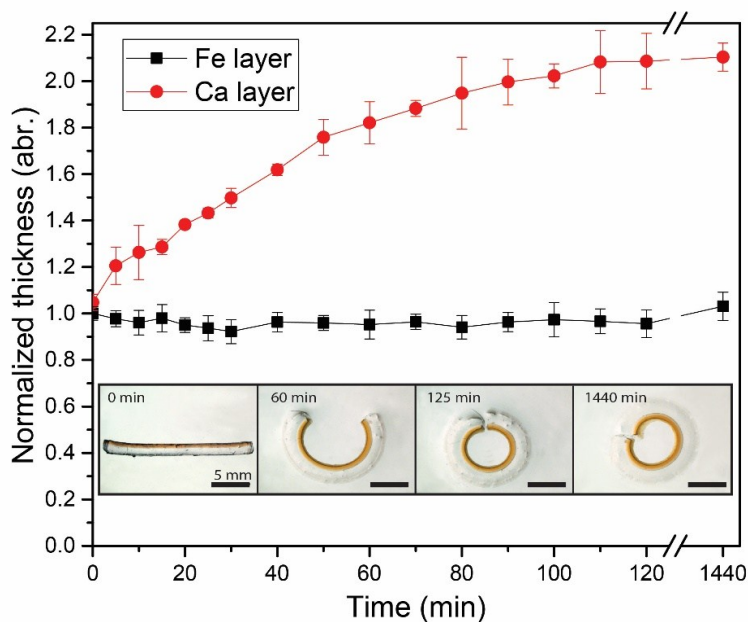


Fig. S3 Thickness evolution of the ferric layer and calcium layer during the swelling-induced bending process.

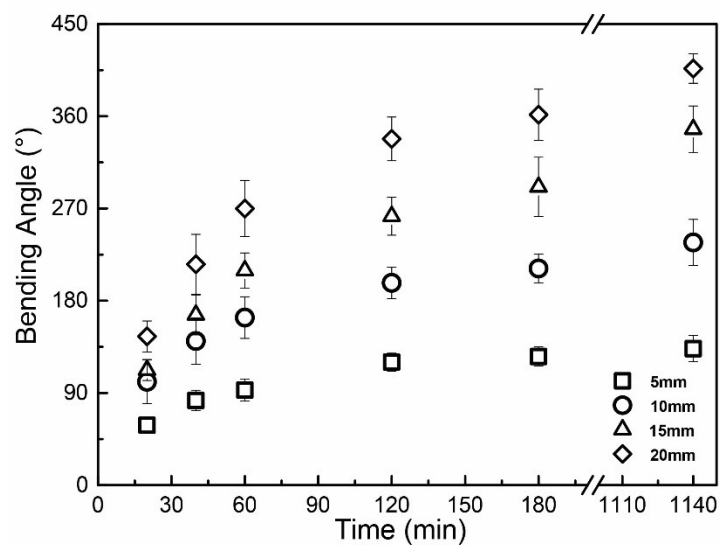


Fig. S4 Bending behavior of the hydrogel strips with different  $\text{Fe}^{3+}$  ion pattern length. The hydrogel strips were patterned with  $\text{Fe}^{3+}$  ions with different length: 5, 10, 15 and 20 mm respectively. The results showed that the longer pattern would induce faster and larger deformation. (Dimensions of the gel strips: 20 mm (long) \* 2 mm (thick) \* 1 mm (wide).)

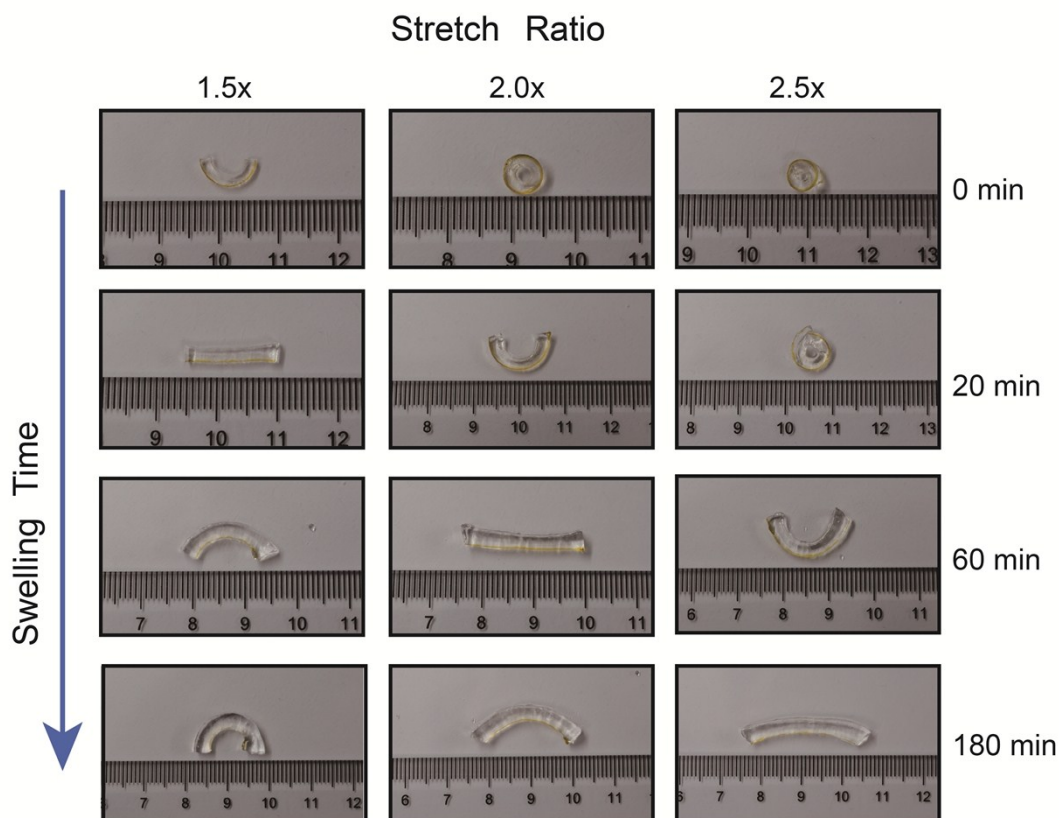


Fig. S5 Dual regulated bending behavior with different stretch ratio and swelling time. The larger stretch would induce larger deformation both from stiffness and swelling mismatch. The tough gel strip with 1.5x stretch first bent to the unpatterned side with  $\sim 180^\circ$  and then bent to the opposite

direction with  $\sim 180^\circ$  after 180 min swelling, which was a good mirror bending. When the gel strip was pre-stretched to 2.5 times its original length, the gel strip would first bend to the unpatterned side up to  $\sim 540^\circ$ , and then bent to the opposite direction with  $\sim 80^\circ$  after 180 min swelling, which was not a mirror bending. However, the overall swelling-induced bending of the gel strip with 2.5x stretch was about  $620^\circ$ , which was larger than that of the 1.5x stretched gel strip ( $180^\circ$ ). (Dimensions of the gel strips: 20 mm (long) \* 2 mm (thick) \* 1.5 mm (wide).)